



OPEN

# Biomimicry of multifunctional nanostructures in the neck feathers of mallard (*Anas platyrhynchos* L.) drakes

Tural Khudiyev<sup>1</sup>, Tamer Dogan<sup>1,3</sup> & Mehmet Bayindir<sup>1,2,3</sup><sup>1</sup>UNAM-National Nanotechnology Research Center, Bilkent University, 06800 Ankara, Turkey, <sup>2</sup>Institute of Materials Science and Nanotechnology, Bilkent University, 06800 Ankara, Turkey, <sup>3</sup>Department of Physics, Bilkent University, 06800 Ankara, Turkey.

Biological systems serve as fundamental sources of inspiration for the development of artificially colored devices, and their investigation provides a great number of photonic design opportunities. While several successful biomimetic designs have been detailed in the literature, conventional fabrication techniques nonetheless remain inferior to their natural counterparts in complexity, ease of production and material economy. Here, we investigate the iridescent neck feathers of *Anas platyrhynchos* drakes, show that they feature an unusual arrangement of two-dimensional (2D) photonic crystals and further exhibit a superhydrophobic surface, and mimic this multifunctional structure using a nanostructure composite fabricated by a recently developed top-down iterative size reduction method, which avoids the above-mentioned fabrication challenges, provides macroscale control and enhances hydrophobicity through the surface structure. Our 2D solid core photonic crystal fibres strongly resemble drake neck plumage in structure and fully polymeric material composition, and can be produced in wide array of colors by minor alterations during the size reduction process.

Nature offers a great diversity of well-optimized photonic engineering designs, which often represent a compromise between several potentially conflicting purposes and can maintain such a diverse array of functions as mate attraction, UV protection, water repulsion, camouflage and sensory enhancement<sup>1,2</sup>. During the last decade, advancements in nanoscience and modern fabrication methods have enabled the detailed investigation and functional mimicry of these natural designs, especially with regards to the structural coloration effects found in biological systems<sup>3–5</sup>. The physical phenomena responsible for structural coloration have also received considerable attention<sup>6,7</sup>, as these structures derive their colors from a number of optical effects, such as interference, scattering, photonic crystal effects, or a combination thereof<sup>8</sup>. Photonic crystals in living systems are especially notable for their iridescence and exceptionally bright coloration<sup>9</sup>, which may assist in camouflage<sup>10,11</sup>, communication<sup>12</sup>, sensing<sup>13–15</sup> and other purposes that still remain largely unexplored. The imitation of these nanostructures represents significant advances<sup>16</sup> in the area of nano-optics, and promotes the design of novel photonic configurations<sup>17,18</sup>. However, current fabrication methods cannot satisfactorily mimic the architectural complexity<sup>19</sup> found in natural systems without greatly compromising control capacity, ease of fabrication and/or production costs. In particular, while nature-inspired 1D and 3D photonic crystals can be fabricated<sup>20,21</sup> by self-assembly or deposition techniques, functional imitations of 2D photonic crystals observed in nature<sup>22–24</sup> are yet to be produced.

Here we investigate and successfully imitate a peculiar 2D photonic scheme observed on the neck feathers of mallard drakes. Our bioinspired 2D photonic crystals successfully replicate not only the optical properties, but also the material features and the architectural complexity of the original structure. A novel top-down approach, called iterative size reduction (ISR)<sup>25–27</sup>, is used to avoid potential issues associated with the fabrication of solid core 2D photonic crystals and to produce a biomimetic design that displays the same structural complexity and functionality as mallard feather barbules with low fabrication costs, short processing times and minimal labor intensity. In addition to its optical properties, the barbule surface is also shown to be strongly hydrophobic, and this property is also successfully replicated in our bio-inspired 2D photonic crystals. The present work represents the first successful fabrication of an all-polymer 2D solid-core photonic crystal capable of functioning at optical frequencies. We further demonstrate that biomimetic fiber arrays displaying a great range of colors can be obtained by minor alterations in a single fabrication step, without necessitating individual process optimization procedures for each desired color.

SUBJECT AREAS:  
PHOTONIC CRYSTALS  
SYNTHESIS AND PROCESSING  
NANOWIRESReceived  
13 January 2014Accepted  
28 March 2014Published  
22 April 2014Correspondence and  
requests for materials  
should be addressed to  
M.B. (bayindir@nano.  
org.tr)

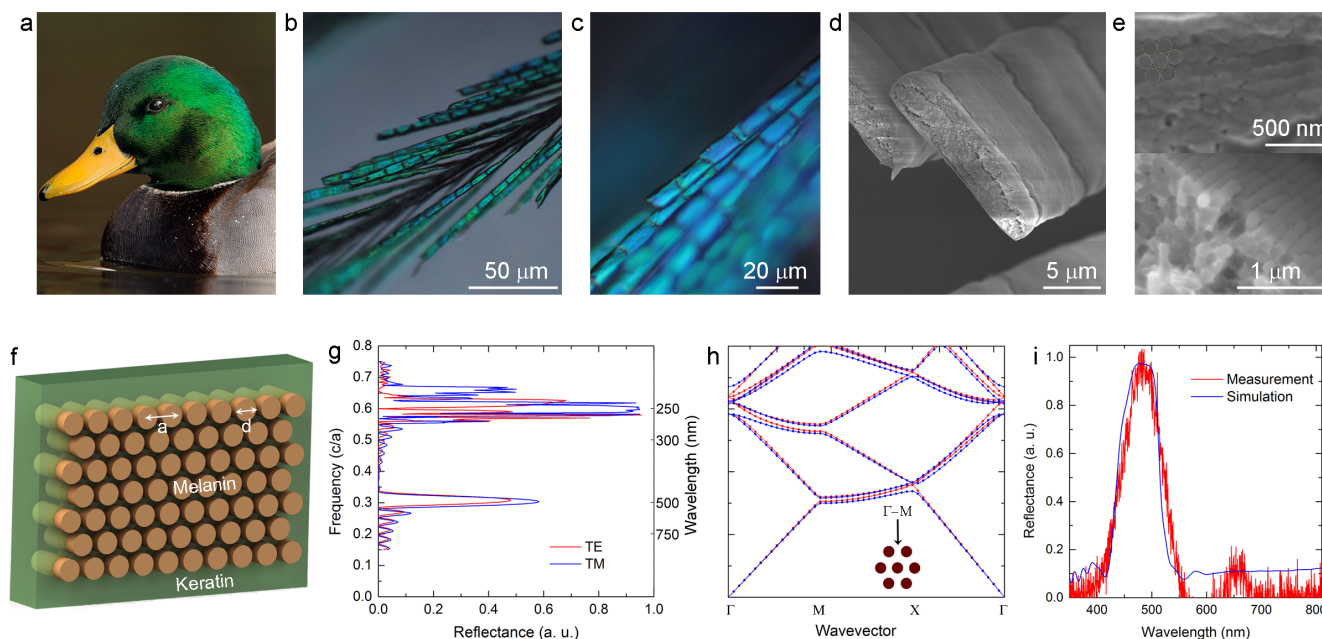


**Figure 1** | Investigation of *A. platyrhynchos* feathers. (a), Mallard neck feathers are investigated for their structural properties (Photographed by Jacob S. Spendelov). Optical microscopy images of mallard neck feathers reveal that higher magnifications result in a change of coloration from (b), green to (c), blue, which suggests the presence of iridescence. Hexagonal arrays of rods are observed from (d), longitudinal and (e), cross-sectional SEM images of feather barbules to be distributed throughout the barbule periphery. (f), Scheme representing the distribution of melanin rods embedded in the keratin matrix. The associated lattice constants (a) and diameters (d) are observed to be around 150 nm and 130 nm, respectively. (g), Reflection simulation of neck feather barbules is performed using the above-mentioned values. (h), Band structure calculations show that directional band-gaps exist in the green and UV regions of the spectrum. (i), Experimental and simulation results associated with the optical features of mallard feathers are in good agreement.

Neck feathers of mallard (*A. platyrhynchos*) drakes (Figure 1a) are investigated to determine the phenomena responsible for their bright green coloration. Optical microscopy characterization suggests that neck feathers are strongly iridescent, as the green hue observed under a low angle of incidence (x20 magnification, Figure 1b) changes into a distinctive blue color when the angle of illumination is increased (x50 magnification, Figure 1c). The barbule morphology possesses a non-circular cross-section, which may serve to maximize the functional surface areas of the barbule elements responsible for iridescent coloration (Figure 1d). Well-aligned, hexagonally distributed rods are observed to occur on barbule edges in five- or six-layer arrays (Figure 1e, Figure S1) and represent an unusual form of 2D photonic crystal<sup>28</sup>. Barbules are primarily composed of melanin pigments (rods) embedded in a keratin matrix (filling material), and display real refractive indices of 2.00 and 1.56, values of which fluctuate slightly over the visible spectrum<sup>29</sup>. Complex refractive index values of these materials play a minor role in coloration by the 2D photonic crystal effect, as they mainly alter the reflected intensity. These fluctuations assumed to be negligible in our calculations.

A moderate refractive index contrast, such as that found in mallard feathers, allows the reflection of a narrow band of wavelengths, the position of which shifts depending on the viewing angle. Consequently, optical simulation techniques were utilized to determine the location and properties of the reflection band associated with barbule elements. Design parameters (Figure 1f) obtained from SEM images of neck feather barbules are used in FDTD and MPB simulations<sup>30</sup>, and the resulting directional band-gap diagram and reflectance spectrum are both found to overlap in the green and ultraviolet regions of the electromagnetic spectrum (Figure 1g–h). The consistency of our simulation and measurement results (Figure S2) further support the notion that the presence of 2D photonic crystals is responsible for the green color displayed by feather barbules (Figure 1i).

The structural orientation of the barbule elements is then utilized in the fabrication of a novel material for use in 2D photonic crystal

based devices. Iterative size reduction is utilized in order to mimic the structural properties observed in mallard feathers, and the size and material data taken from feather barbules are used to simplify the design process. Polycarbonate (PC) and polyvinylidene difluoride (PVDF) are selected as the material components due to their thermal compatibility, which is required for the thermal drawing process, and low refractive index contrast ( $n_{PC}=1.58$  and  $n_{PVDF}=1.41$ ), which closely approximates the original configuration (Figure S3). The first step macroscopic preform (Figure 2a, Figure S4a, b) is prepared by successively wrapping PVDF and PC polymers around a PC rod, which is then thermally consolidated in a furnace (see Methods). The final macrostructure measures several centimeters in diameter, and is thermally drawn in a custom-built fibre tower system to effect the iterative reduction of structure dimensions (see Ref. 25 for details). Fabricated step I fibres (Figure 2d) possess an excellent cross-sectional regularity that is preserved along the length of the fibre. Microstructures obtained after step I are cut and prepared for the second step of the fabrication (Figure 2b).

Composite fibres with outer diameters of several hundred microns are embedded in a polymer sheath (*i.e.* a rectangular hollow preform prepared for the insertion of first step microfibrils) (Figure S4c, d) in self-arranged hexagonal arrays and redrawn to produce indefinitely long 2D photonic crystal microstructures. Microwave arrays present within the PVDF matrix of step II fibres preserve their initial structure profile, as can be observed from their cross-section images (Figure 2e). A third step, similar in procedure to step II but utilizing only one step II fibre, can then be performed to produce step III fibres with nano- to microscale lattice constants (Figure 2c). Microstructures with rectangular cross-sections composed of hexagonal arrays of nanorods are obtained after three consecutive drawing steps, and bear a great resemblance to the fine structure of mallard feathers. 2D photonic crystal structures obtained as a result of step II and step III fabrications span a wide range of lattice sizes (50  $\mu\text{m}$ –100 nm).

SEM images of step III fibres are relatively low-quality due to the low contrast between the photonic crystal components (Figure 2f).

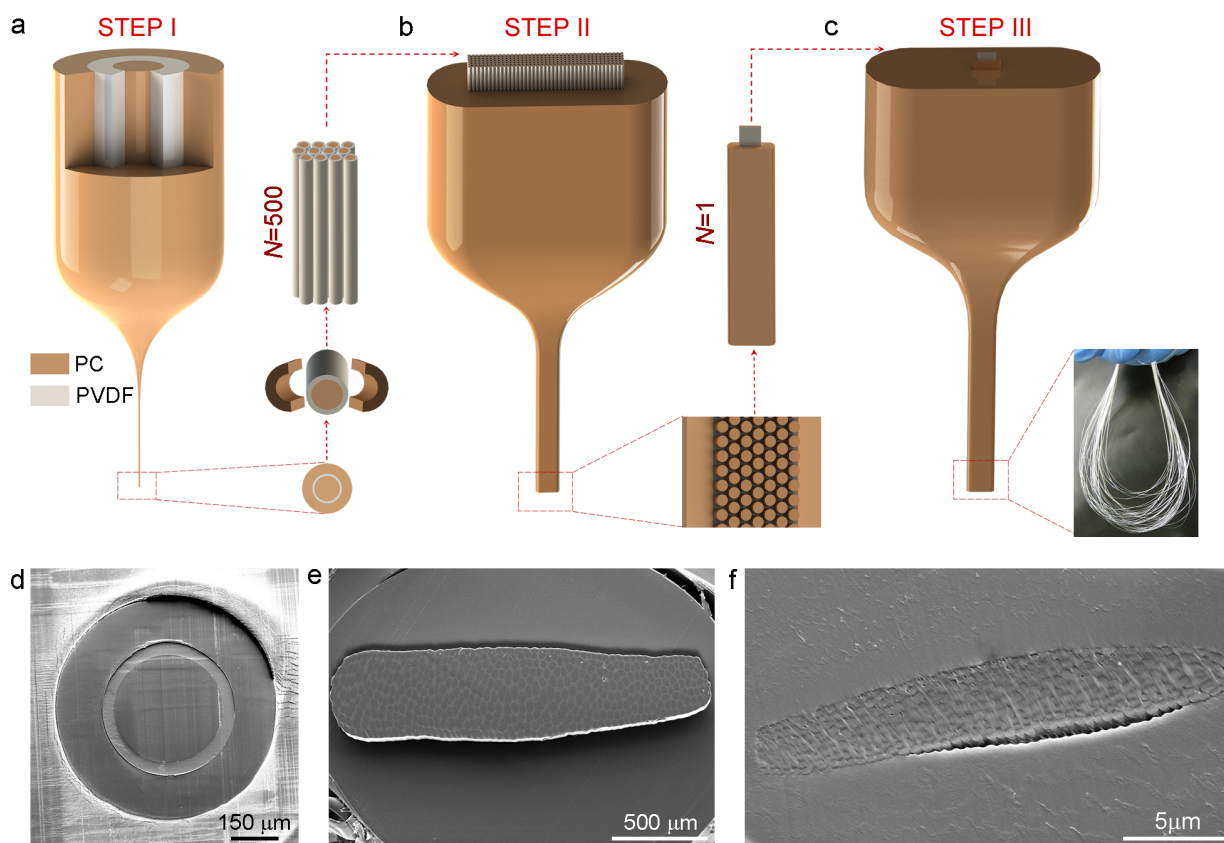


**Figure 2 | Functional biomimetics of mallard drake feathers.** A low temperature, multimaterial fibre drawing method is used for the iterative reduction of a macroscopic preform down to microscale photonic crystal. (a), The first step preform is obtained by successively wrapping PVDF and PC polymer films around a PC rod. The outer layer of step I fibres removed prior to the second step of fabrication. (b), In the second step, a rectangular formation is used in order to increase the aspect ratio of the final result, so as to resemble the design observed in *A. platyrhynchos* feathers. PVDF embedded PC microwires with lattice constants of several microns are produced at the end of step II. (c), Step III is performed by repeating previous fabrication procedures, and permits the precise control of the lattice constant in the 100–300 nm region. (d–f), Cross-sectional SEM images of produced fibers after steps I, II and III, respectively.

Minor deformations observed in rod structures may slightly alter the local hue, but do not significantly change the overall color.

Our multiple size reduction process can therefore be utilized to convert the white-colored macro-prototype into structurally colored photonic crystal fibres (Figure 3a). The green hue observed in optical microscope images of 2D all-polymer photonic crystal structures (Figure 3b) shifts into blue under higher magnifications as a result of its iridescence (Figure 3c). Longitudinal SEM images reveal that the PVDF shell acts as an embedding matrix for PC nanorods (Figure 3d). Roughnesses are observed to exist on the photonic crystal surface, but are too small to display Mie scattering or thin film interference, and are therefore expected to play an insignificant role in coloration<sup>26,31</sup>. Lattice constants and rod diameters are measured to be around 200 nm and 175 nm for green-colored 2D photonic crystal fibres. The reflection spectra and band structure behavior of produced fibres can be simulated accurately by using these values (Figure 3f, g). Our measurement and unpolarized light simulation data are also in good agreement for green-colored fibres (Figure 3h).

Our bioinspired solid-core 2D photonic crystal fibres are also used for the production of a diverse array of colored fibres spanning the visible spectrum. Decreasing lattice constants and rod diameters gradually change the hues observed on a tapered part of photonic crystal fibre (Figure 4a). A 3D map of the photonic crystal effect clearly demonstrates band-gap positions associated with specific lattice constants, and can assist in the design of colored photonic crystal fibres (Figure 4b). Narrow reflection bands allow the clear observation of each color. The reduction factor can be altered during the

third step of the drawing process to modify the lattice constant of the final product and to facilitate the single-step fabrication of arbitrarily long, structurally colored photonic crystal fibres (Figure 4c).

Mallard neck feathers (unlike flight feathers<sup>32</sup>) and our bio-inspired photonic 2D crystal fibres are both found to be strongly hydrophobic due to their similar surface architectures, though different effects are responsible for their enhanced hydrophobicities (Figure 5). SEM images of feather barbules suggest that three surface effects contribute to feather hydrophobicity ( $CA = 152^\circ \pm 2^\circ$ ): (1) The gaps present within the barbule arrays, (2) the interlocking steps between each barbule cluster and (3) the nanoscale roughness of each barbule surface (Figure 5a,b)<sup>33</sup>. Similarly, the surface nanopattern and arrangement of our photonic crystal fibres, as well as the intrinsically hydrophobic nature of the PVDF polymer shell, contribute to the superhydrophobicity of our bio-inspired photonic crystals (Figure 5c,d). PVDF is a fluoride-containing polymer, and fluorinated residues are well-known to promote hydrophobicity<sup>34</sup> (Figure S5a). However, our all-polymer step III photonic crystal structures ( $CA = 160^\circ \pm 5^\circ$ ) are more hydrophobic than PVDF polymer films ( $CA = 91^\circ$ ), suggesting that, in addition to material composition, surface hierarchy also contributes significantly to the superhydrophobicity of the fibrous photonic crystal surfaces (Figure 5e). Higher hydrophobicities are also observed for step II fibres ( $CA = 124^\circ$ ), which possess microscale surface patterns, as opposed to the nanoscale features of step III fibres (Figure S5b).

The polymeric composition of our 2D photonic crystal design also confers additional features such as biocompatibility, elasticity and

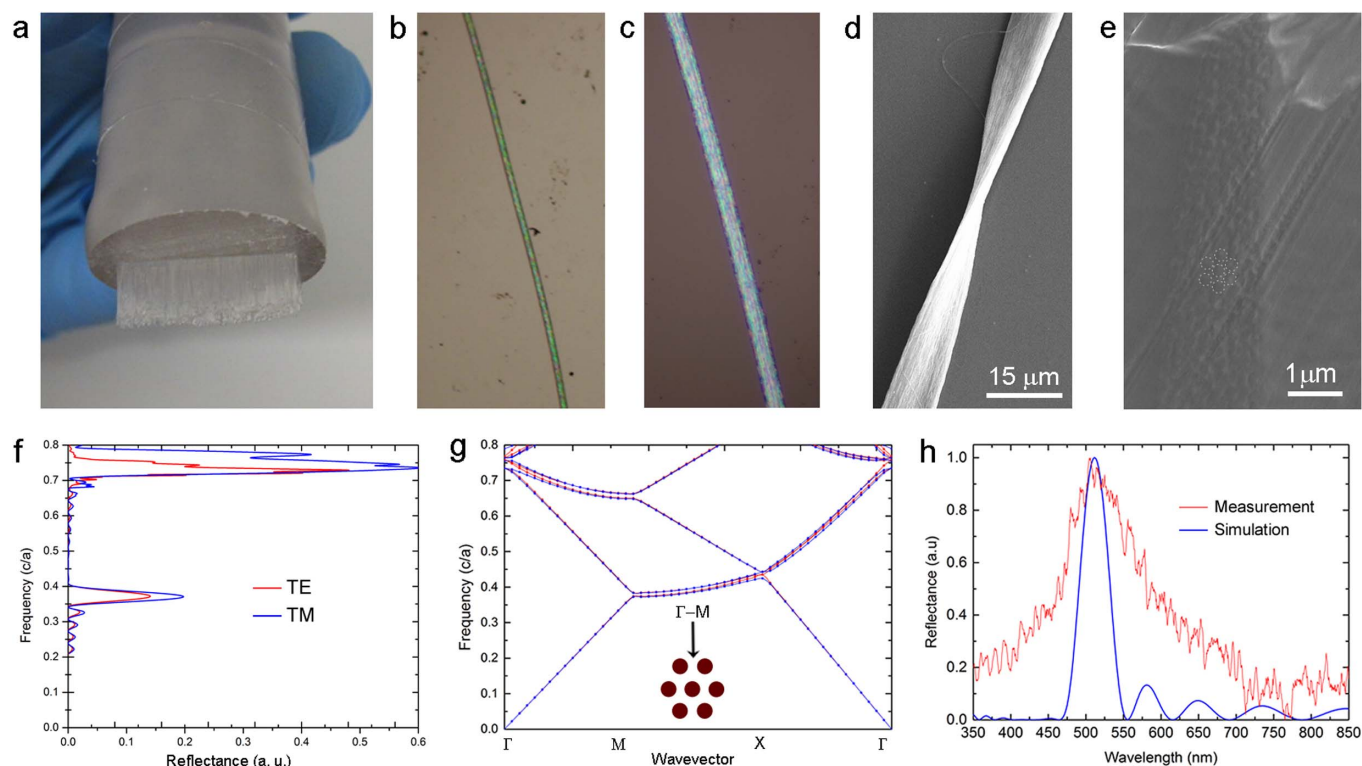


**Figure 3 | Characterization of biomimetic all-polymer photonic crystal structures.** (a), A diverse array of 2D photonic crystal nanostructures can be engineered from a unique macroscale preform. (b), The vivid green hue observed under light microscopy confirms the presence of photonic crystal effects. (c), Biomimetic photonic crystal fibres appear iridescent as the magnification of light microscope is increased. The green color is transformed into blue as a result of the photonic crystal effect. (d–e), SEM images reveal the ribbonlike photonic crystal formation and hexagonal distribution of PC rods inside the PVDF matrix, with lattice constants around 200 nm. (f), Reflection and (g), bandstructure calculations are performed using the optical and size parameters of the material components. (h), Reflection measurements from green colored photonic crystal structures are consistent with FDTD modelling results.

pliability to structurally colored fibres<sup>35–38</sup>. These fibres can also be produced in millimeter to nanometer scales, and can therefore be utilized on different operation wavelengths (i.e., UV, visible and IR). In addition, our fabrication method allows the precise control of the fibre production process, and therefore can effectively facilitate the fabrication of a broad range of complex nanoarchitectures. The

fabrication of hard-to-produce 2D photonic crystal structures with distinct material compositions can also be accomplished by choosing thermally compatible raw materials<sup>22,23</sup>. Such photonic crystal fibers are promising for use in applications relating to filtering<sup>39</sup>, colored fabric woven<sup>40,41</sup> and their superhydrophobic character is particularly useful in anisotropic wettable fibers<sup>42</sup>.

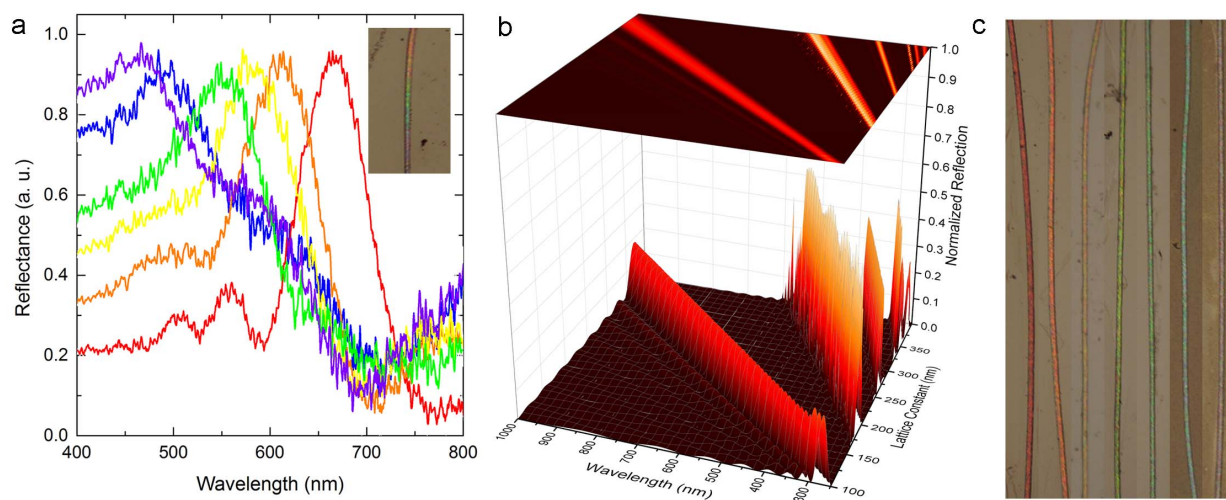


**Figure 4 | Band-gap tunable all-polymer colorful photonic crystal structures.** (a), A tapered photonic crystal structure exhibits lattice constant-dependent changes in color along 200  $\mu\text{m}$  of its length. Measurements are taken from each hue observed on the tapered photonic crystal (inset). (b), A map of bandstructure calculations can be used in the design of any desired color. (c), A large array of colors can also be obtained during the third fabrication step by altering the reduction factor. Millimeter-scale structures displaying seven distinct colors are shown as a proof-of-concept.

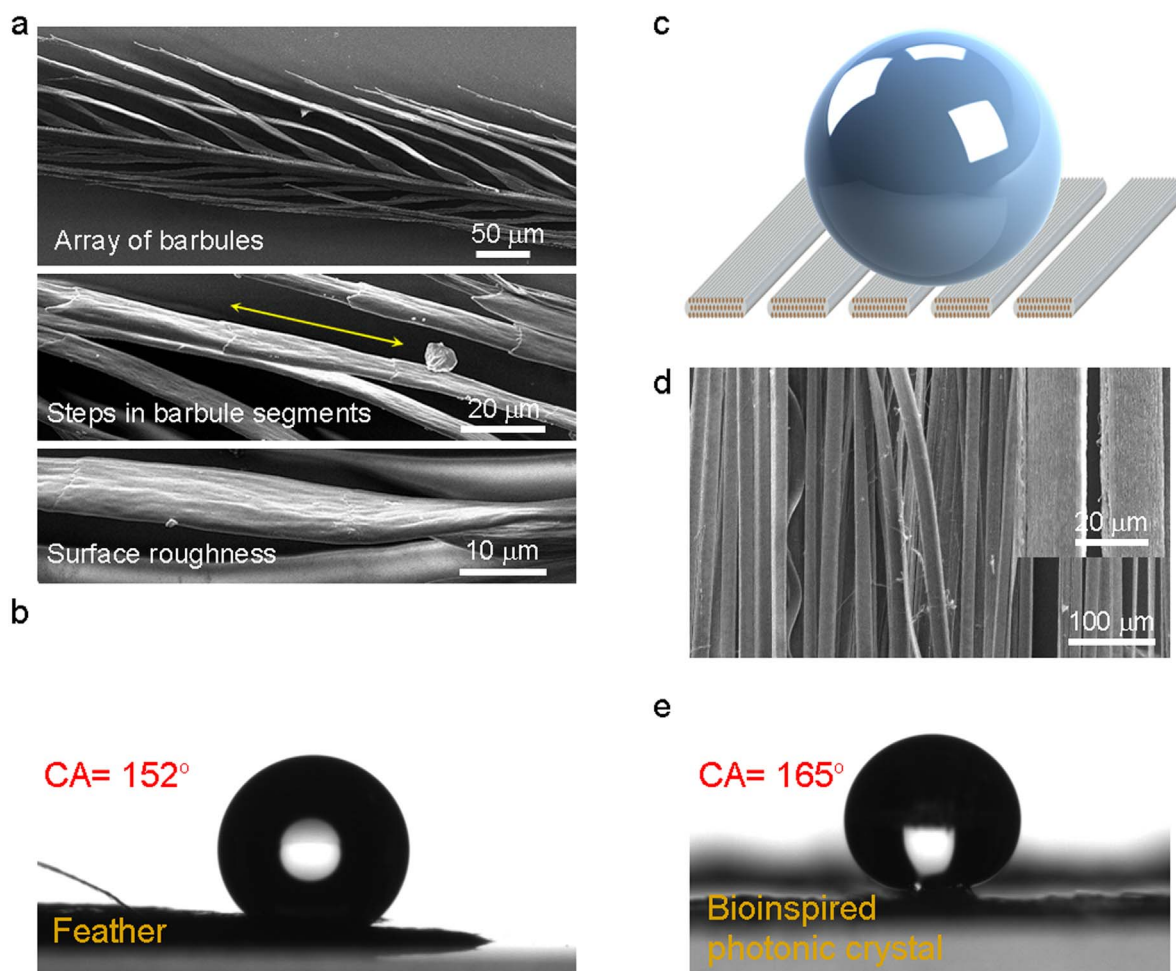


**Figure 5 | Enhanced hydrophobicity in feather and feather-inspired photonic crystal structure.** (a), Neck feathers exhibit superhydrophobicity due to presence of structural hierarchy. (b), Contact angle measurement of a single mallard feather. (c), Our photonic crystal surface enhances the intrinsic hydrophobicity of PVDF film (see Figure S5) by increasing surface roughnesses. (d), The nanoscale surface pattern observed on step III structures and the alignment of the fiber arrays both contribute to surface superhydrophobicity. (e), The water contact angle is measured to exceed  $165^\circ$  for this particular array.

## Methods

### Macroscopic composite preparation, consolidation and thermal size reduction.

Photonic crystals are produced using three iterative fabrication steps. A single step I preform is utilized throughout the fabrication process, and uses a PC rod as a core component, which in turn is prepared using a hollow PC preform with an initial diameter of 30 mm. Briefly, the PC preform is cut into four equal pieces, and a turning machine is used to shape a single quadrant into a cylindrical rod with a diameter of 10 mm. A PVDF polymer film is then wrapped around this rod until a total diameter of 12 mm is reached, and a PC film is wrapped around the PC/PVDF core until the total diameter exceeds 20 mm (the complete preform therefore has a diameter ratio of 10 : 2 : 8 for PC : PVDF : PC).

The macroscopic preform is then consolidated above the glass transition temperature of its components ( $185^\circ\text{C}$  for 10 minutes, under a  $10^{-3}$  Torr vacuum), and thermally drawn in a custom-built fibre tower, specifications of which can be found in Ref 25. Briefly, the macroscopic structure is heated and drawn into step I microwires in a vertical two-zone furnace, with a top zone temperature of  $224^\circ\text{C}$ . Drawing parameters, such as drawing speed, down feed speed and temperature, are controlled throughout the fabrication process. Fibres with outside diameters of 400  $\mu\text{m}$  are obtained as a result of step I fabrication, and the outer coat of PC is stripped prior to the subsequent steps (the non-adhesive layer between PVDF and PC facilitates the convenient removal of PC).

Functional biomimicry of the rectangular photonic crystal structures observed in mallard feathers is accomplished using a rectangular step II preform (step II preforms are hollow PC structures into which step I fibres are inserted). The rectangular step II preform is prepared by wrapping PC film around a bare glass substrate with the dimensions of 20 mm  $\times$  1.5 mm  $\times$  7 cm, to a final thickness of 35 mm  $\times$  15 mm  $\times$  7 cm. This preform is then thermally consolidated in a consolidation furnace, with an extended heating time ( $>2$  h) to ensure that the outer PC layer conforms fully to the shape of the glass rod. The glass rod is then dissolved using 48% HF, leaving behind the rectangular preform. A 4cm-long array of 500 step I fibres is inserted into this step

II preform and thermally drawn at a temperature of  $230^\circ\text{C}$  in our custom fibre tower system (see also Ref. 25 for other parameters used in the fibre drawing process, such as capstan and down-feed speed). Fibres with outside diameters of 1.5 mm are obtained at the end of the second step. Step III is identical to step II, except that step III preforms are filled with a single step II fibre. Arbitrarily long photonic crystals can be produced with a broad crystal parameter range (including lattice constant  $> 100$  nm) after step III, and the process can be repeated to obtain smaller structure diameters. The overall reduction factor at the end of step III is  $10^5$ .

**Sample preparation and imaging.** Dichloromethane (DCM) (Carlo Erba) is utilized to etch the PC sheath covering the photonic crystal structures, exposing the latter for longitudinal imaging by electron and optical microscopy. Exposed nanostructures are rinsed gently with DCM for the removal of residual polymer. PVDF shells of photonic crystal structures are highly resistant to DCM etching, and are not damaged during the nanostructure extraction process. Cross-sectional images of mallard feathers and bio-inspired photonic crystals were obtained by embedding both structures in epoxy resin and sectioning them by ultramicrotome prior to imaging. Cross-sectional images are difficult to obtain due to the low contrast between the material components of both feather barbules and our bio-inspired fibres. SEM imaging is performed under both high pressure and low pressure modes to minimize this problem.

**FDTD simulations and MPB calculations.** FDTD simulations are performed by using commercial finite-difference time-domain software (Lumerical Solutions Inc.). A planewave source is used for illumination. FDTD simulations are calculated in two dimensional simulation regions. Frequency-domain power monitors are used to collect reflected light from periodic layers of rods embedded in host material. Refractive indices of PC and PVDF are assumed to be constant in the visible spectrum, and taken as 1.58 and 1.41 (see Figure S3).



(MIT Photonic-Bands) MPB is an open-source code developed by MIT for the computation of photonic band structures. For our work, triangular lattice configurations were used for the calculations involving both feather barbules and barbule-mimetic photonic crystal structures, radius to lattice ( $r/a$ ) ratios of which were measured from SEM images to be 0.4330 and 0.4375, respectively.

- Liu, K. & Jiang, L. Bio-inspired design of multiscale structures for function integration. *Nano Today* **6**, 155–175 (2011).
- Duprat, C., Protière, S., Beebe, A. Y. & Stone, H. A. Wetting of flexible fibre arrays. *Nature* **482**, 510–513 (2012).
- Fudouzi, H. Tunable structural color in organisms and photonic materials for design of bioinspired materials. *Sci. Technol. Adv. Mater.* **12**, 064704 (2011).
- Finnemore, A. *et al.* Biomimetic layer-by-layer assembly of artificial nacre. *Nature Commun.* **3**, 966 (2012).
- Kolle, M. *et al.* Mimicking the colourful wing scale structure of the *Papilio blumei* butterfly. *Nature Nanotechnol.* **5**, 511–515 (2010).
- Vukusic, P., Sambles, J. R. & Lawrence, C. R. Structural colour: Colour mixing in wing scales of a butterfly. *Nature* **404**, 457 (2000).
- Whitney, H. M. *et al.* Floral iridescence, produced by diffractive optics, acts as a cue for animal pollinators. *Science* **323**, 130–133 (2009).
- Kinoshita, S. & Yoshioka, S. Structural colors in nature: the role of regularity and irregularity in the structure. *ChemPhysChem* **6**, 1442–1459 (2005).
- Vukusic, P., Sambles, J. R., Lawrence, C. R. & Wootton, R. J. Structural colour: Now you see it —now you don't. *Nature* **410**, 36 (2001).
- Wiersma, D. S. Disordered photonics. *Nature Photon.* **7**, 188–196 (2013).
- Wilts, B. D. *et al.* Brilliant camouflage: photonic crystals in the diamond weevil, *Entimus imperialis*. *Proc. R. Soc. B* **279**, 2524–2530 (2012).
- Ghiradella, H. Light and color on the wing: Structural colors in butterflies and moths. *Appl. Opt.* **30**, 3492–3500 (1991).
- Potyrailo, R. A. *et al.* Morpho butterfly wing scales demonstrate highly selective vapour response. *Nature Photon.* **1**, 123–128 (2007).
- Kim, J. H., Moon, J. H., Lee, S. Y. & Park, J. Biologically inspired humidity sensor based on three-dimensional photonic crystals. *Appl. Phys. Lett.* **97**, 103701 (2010).
- Sambles, J. R. Biophotonics: Blue butterflies feel the heat. *Nature Photon.* **6**, 141–142 (2012).
- Parker, A. R. & Townley, H. E. Biomimetics of photonic nanostructures. *Nature Nanotechnol.* **2**, 347–353 (2007).
- Pris, A. D. *et al.* Towards high-speed imaging of infrared photons with bio-inspired nanoarchitectures. *Nature Photon.* **6**, 195–200 (2012).
- Walish, J. J., Kang, Y., Mickiewicz, R. A. & Thomas, E. L. Bioinspired electrochemically tunable block copolymer full color pixels. *Adv. Mater.* **21**, 3078–3081 (2009).
- Vukusic, P. & Sambles, J. R. Photonic structures in biology. *Nature* **424**, 852–855 (2003).
- Diao, Y. Y. & Liu, X. Y. Controlled colloidal assembly: Experimental modeling of general crystallization and biomimicking of structural color. *Adv. Func. Mater.* **22**, 1354–1375 (2012).
- Kolle, M. *et al.* Bio-inspired band-gap tunable elastic optical multilayer fibres. *Adv. Mater.* **25**, 2239–2245 (2013).
- Zi, J. *et al.* Coloration strategies in peacock feathers. *Proc. Natl. Acad. Sci.* **100**, 12576–12578 (2003).
- Vigneron, J. P. *et al.* Structural origin of the colored reflections from the black-billed magpie feathers. *Phys. Rev. E* **73**, 021914 (2006).
- Eliason, C. M. & Shawkey, M. D. A photonic heterostructure produces diverse iridescent colours in duck wing patches. *J. R. Soc. Interface* **9**, 2279–2289 (2012).
- Yaman, M. *et al.* Arrays of indefinitely long, uniform nanowires and nanotubes. *Nature Mater.* **10**, 494–501 (2011).
- Khudiyev, T., Ozgur, E., Yaman, M. & Bayindir, M. Structural coloring in large scale core-shell nanowires. *Nano Lett.* **11**, 4661–4665 (2011).
- Ozgur, E., Aktas, O., Kanik, M., Yaman, M. & Bayindir, M. Macroscopic assembly of indefinitely long and parallel nanowires into large area photodetection circuitry. *Nano Lett.* **12**, 2483–2487 (2012).
- Joannopoulos, J. D., Johnson, S. G., Winn, J. N. & Meade, R. D. *Photonic crystals: Molding the flow of light*. Princeton University Press. (2011).
- Brink, D. J. & van der Berg, N. G. Structural colours from the feathers of the bird *Bostrychia hagedash*. *J. Phys. D: Appl. Phys.* **37**, 813–818 (2004).
- Johnson, S. G. & Joannopoulos, J. D. Block-iterative frequency-domain methods for Maxwell's equations in a planewave basis. *Opt. Express* **8**, 173–190 (2001).
- Khudiyev, T., Huseyinoglu, E. & Bayindir, M. Non-resonant Mie scattering: Emergent optical properties of core-shell polymer nanowires. *Sci. Rep.* **4**, 4607 (2014).
- Eliason, C. M. & Shawkey, M. D. Decreased hydrophobicity of iridescent feathers: a potential cost of shiny plumage. *J. Exp. Biol.* **214**, 2157–2163 (2011).
- Oner, D. & McCarthy, T. J. Ultrahydrophobic surfaces. Effects of topography length scales on wettability. *Langmuir*, **16**, 7777–7782 (2000).
- Biffinger, J. C., Kim, H. W. & DiMango, S. G. The polar hydrophobicity of fluorinated compounds. *ChemBioChem* **5**, 622–627 (2004).
- Qi, Y. & McAlpine, M. C. Nanotechnology-enabled flexible and biocompatible energy harvesting. *Energ. Environ. Sci.* **3**, 1275–1285 (2010).
- Holmes-Siedle, A. G., Wilson, P. D. & Verrall, A. P. PVdF: An electronically-active polymer for industry. *Mater. Design.* **4**, 910–918 (1984).
- Nakazawa, M., Shi, Y. W., Matsuura, Y., Iwai, K., & Miyagi, M. Hollow polycarbonate fiber for Er: YAG laser light delivery. *Opt. Lett.* **31**, 1373–1375 (2006).
- Han, M., Hyun, D. H., Park, H. H., Lee, S. S., Kim, C. H., & Kim, C. A novel fabrication process for out-of-plane microneedle sheets of biocompatible polymer. *J. Micromech. Microeng.* **17**, 1184–1191 (2007).
- Stecher, M. *et al.* Polymeric THz 2D photonic crystal filters fabricated by fiber drawing. *IEEE Trans. Terahertz Sci. Technol.* **2**, 203–207 (2012).
- Abouraddy, A. F. & Bayindir, M. *et al.* Towards multimaterial multifunctional fibres that see, hear, sense and communicate. *Nature Mater.* **6**, 336–347 (2007).
- Gauvreau, B. *et al.* Color-changing and color-tunable photonic bandgap fiber textiles. *Opt. Express* **16**, 15677–15693 (2008).
- Wu, H. *et al.* Biomimetic nanofiber patterns with controlled wettability. *Soft Matter*, **4**, 2429–2433 (2008).

## Acknowledgments

We would like to thank to Ekin O. Ozgur for her help in obtaining SEM images of mallard drake feathers, and Alper D. Ozkan for his critical reading of the manuscript and fruitful discussions. This work is supported by TUBITAK under the Project Nos. 110M412 and 111A015. The research leading to these results has received funding from the European Research Council under the European Union's Seventh Framework Programme (FP/2007-2013)/ERC Grant Agreement n. 307357. M.B. acknowledges partial support from the Turkish Academy of Sciences (TUBA).

## Author contributions

T.K., T.D. and M.B. designed and carried out research, analyzed data and wrote the paper.

## Additional information

Supplementary information accompanies this paper at <http://www.nature.com/scientificreports>

**Competing financial interests:** The authors declare no competing financial interests.

**How to cite this article:** Khudiyev, T., Dogan, T. & Bayindir, M. Biomimicry of multifunctional nanostructures in the neck feathers of mallard (*Anas platyrhynchos* L.) drakes. *Sci. Rep.* **4**, 4718; DOI:10.1038/srep04718 (2014).



This work is licensed under a Creative Commons Attribution-NonCommercial-ShareAlike 3.0 Unported License. The images in this article are included in the article's Creative Commons license, unless indicated otherwise in the image credit; if the image is not included under the Creative Commons license, users will need to obtain permission from the license holder in order to reproduce the image. To view a copy of this license, visit <http://creativecommons.org/licenses/by-nc-sa/3.0/>